



Dried sewage sludge as an efficient adsorbent for pollutants: cationic methylene blue removal case study

Youssef Aoulad El Hadj Ali¹ · Mohammadi Ahrouch^{2,3} · Abdellatif Ait Lahcen⁴ · Abdoulaye Demba N'diaye⁵ · Farida El Yousfi¹ · Mostafa Stitou¹

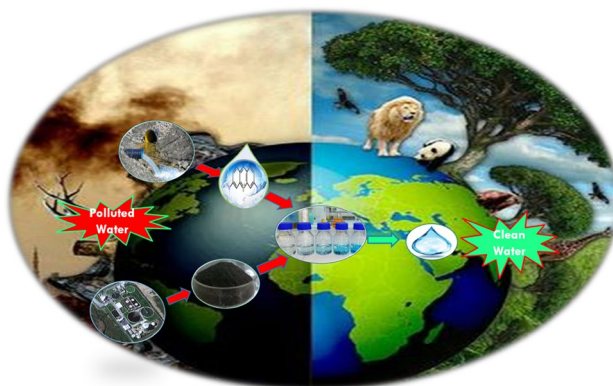
Received: 1 December 2020 / Accepted: 27 February 2021
© The Author(s), under exclusive licence to Springer Nature Switzerland AG 2021

Abstract

Sewage sludge valorization must be the favored solution of management for a residue that does not present the desired improvement in terms of wastewater treatment. The objective of this research work was to study the dye fixation capacity of the adsorbents produced from sewage sludge. The dried sewage sludge (DSS) was used as an adsorbent to remove a cationic dye, methylene blue (MB), from an aqueous solution in a batch system, as a function of contact time, pH, temperature and initial concentration. The proposed adsorbent was characterized using several techniques such as scanning electron microscopy (SEM), Brunauer–Emmett–Teller (BET) analysis, X-ray diffraction (XRD) and Fourier Transform Infrared Spectroscopy (FTIR). The adsorption equilibrium of MB was described using Langmuir, Freundlich and Sips equations. The equilibrium is perfectly adapted to the Langmuir model with a maximum adsorption capacity of 44.39 mg g^{-1} on a single layer. In order to study the adsorption mechanisms, first- and second-order kinetic models were used. The adsorbent produced from the sludge was capable of absorbing MB from the solution, with the expression of the second-order rate being preferred to that of the first order. In addition, the thermodynamic parameters were evaluated, demonstrating that the adsorption process is spontaneous and endothermic. Thus, this study convinced that the DDS proved to be an alternative, attractive, effective, economic, and environmentally friendly adsorbent for MB dye removal from aqueous solution.

Graphic abstract

Schematic illustration of the prepared dried sewage sludge adsorbent for the removal of methylene blue from aquatic samples



Keywords Dried Sewage Sludge · Methylene bleu · Adsorption · Wastewater treatment plant · Emerging contaminants

✉ Youssef Aoulad El Hadj Ali
aouladelhadjali@uae.ac.ma

✉ Mostafa Stitou
stitou.mostafa@uae.ac.ma

Extended author information available on the last page of the article

Introduction

Sewage sludge a by-product of the wastewater treatment plants (WWTPs), is considered as a part of the urban or industrial waste [1]. Therefore, this type of waste can be recovered and reused in various fields including energy and agriculture [2–4]. From an economic and environmental point of view, any waste becomes less constraining if it can be reused, especially if there is an opportunity to recycle it, this helps in reducing water and air pollution as well as the consumption of energy and raw materials [5, 6]. Recently, as stated in international environmental standards, the amount of sewage sludge produced by WWTPs increase, which is mainly due to the demographic growth accompanied with a strong industrialization and urbanization [7–10]. According to the Moroccan environmental policy, the amount of wastewater treated and sewage sludge (SS) produced in the country is systematically increasing [11, 12]. In fact, the implicit objectives of the National Program of Sanitation Liquid and Wastewater Treatment jointly by the Department of the Environment include the improvement of water quality in the natural environment and the possibility of reusing treated wastewater [13]. Otherwise, they are focused on the objectives of protecting the environment and human health.

The treatment and recovery of SS are crucial points in the water cycle as well as in environmental protection. Therefore, the main sludge treatment routes are digestion, landfilling and incineration [14]. Moreover, several countries in the Mediterranean region are situated in semi-arid to arid climates, like North African countries, with a significant water supply deficit [15–18]. The treated water obtained is reused for agriculture and irrigation after each treatment. In this regard, the development of adsorbents based on urban SS, economically profitable and efficient for the treatment of ecosystems, by the different processes of adsorption or photo catalysis are among the subjects of current research that arouse the interest of several researchers worldwide [19–21]. The direct or indirect discharge of wastewater containing organic compounds into the environment has increased with the fast development of certain human and industrial activities such as the textile, tanning and pharmaceutical industries [22]. In this sense, the release of natural or synthetic pollutants such as laundry detergents, organic compounds dyes [23, 24], and antibiotics in the environment are tremendously increasing [25, 26]. It has been reported that approximately 10–20% of the dyes applied in textile activities are released directly into the environment in the form of aqueous effluents [27, 28]. In addition, these emerging pollutants are less or non-biodegradable. Indeed, their toxicological impact on the health and the environment is highly significant

and very harmful [29, 30]. Hence, the development of new strategies for the removal of these toxic pollutants from wastewater is highly needed. The implementation of an efficient and reliable disposal technique becomes important to obtain treated water of appropriate quality for human activity and to protect environment. In this context, several developed techniques have been employed and investigated for the removal of organic compounds dyes (MB as cationic model dyes), such as chemical precipitation, advanced oxidation process [31], ion exchange [32], membrane filtration [33, 34], photocatalytic degradation [35], and adsorption processes [36, 37]. However, the adsorption process is one of the effective methods among all the above-mentioned ones for the removal of MB from wastewater. This is due to their versatility and the growing availability of various types of eco-friendly and low-cost adsorbents like Grass waste, Papaya seeds and Water hyacinth [38].

Recently, many materials have been investigated to determine their adsorption capacity for cationic methylene blue (MB) dye, such as, natural phosphate, zeolite, clay minerals (naturel, modified and extruded) [39], lignite [40] and activated carbon [20]. In this context, several sludge-based activated carbons has been also successfully reported to eliminate MB and other cationic dyes in wastewater [41]. Therefore, the major drawback of this kind of adsorbents is their high-cost, and difficulties of reusability. However, the development of cost-effective and reusable sorbent materials with greater efficiency for the removal of aquatic contaminants is highly needed. Therefore, in this study we aimed to investigate an effective, easy and rapid approach to valorize the sewage sludge into environmentally friendly adsorbents. Then, the adsorption efficiency of cationic methylene blue (MB) dye on a dried sewage sludge (DSS) was evaluated in a batch study. Indeed, the influence of adsorbent dosage, pH value, ionic strength, contact time and temperature effect. The kinetic and isotherm equilibrium models were combined with thermodynamic parameters to further explore the interaction adsorption mechanisms.

Otero et al. have reported the adsorption of MB using different adsorbent produced from sewage sludges. The kinetic studies have been carried out using conventional models of Langmuir and Freundlich isotherms. Their results showed that DSS demonstrated high adsorption capacity towards the removal of MB [42]. In the same context, Dhaouadi et al. reported the use of sewage sludge as a textile vat dye adsorbent. Their adsorbent exhibited an excellent performance with a good dye retention capacity that varies from 60 to 75 mg/g following both Langmuir and Freundlich isotherm models [43].

In this research work, the MB was selected taking into account the extensive literature reported on the use of this cationic dye in liquid phase adsorption studies, using

different adsorbent materials. Furthermore, it was also chosen for its significant presence in wastewater from the local Moroccan textile industry. Certainly, other dyes could also be interesting to adsorb, such as Crystal violet, Rhodamine B, Congo red, among others. However, MB is the most studied, due to its widespread use in many industries.

Experimental

Preparation and characterization of adsorbent

In this study, the raw sludge samples were collected during the summer, from the WWTP Tamuda bay (Mdiq-Fnideq/Morocco). 7 L of Sample which about 6.70 kg of the sample carried out in PVC recipients are inert to sludge, resistant to moisture and impervious to water and dust. The sample taken was a fresh solid has a dark black colour. It was dried at 40 °C in an oven for overnight, then crushed in a mortar then analysed using granulometry analysis grain size (Endecotts Ltd, Lombard Road, London, SW, 93BR England, Telex: 929395) to obtain fine particles of DSS, characterized by a diameter between $0.5 \text{ mm} \leq d < 3 \text{ mm}$. After that, the DSS powder obtained is packaged in small boxes and stored in a desiccator until further use.

In order to identify the crystalline structures, the powder X-ray diffraction (XRD) pattern was performed in a Bruker diffractometer (Phillips Xpert-pro model), using Cu K α $\lambda = 1.54051 \text{ \AA}$ radiation with a step of $0.017^\circ/1 \text{ s}$. In addition, a semi-quantitative analysis of the mineralogical composition was performed using the Powder Cell 2.4 software D8 Advance 500 model.

Fourier transform infrared (FTIR) spectroscopy (Thermo Vertex 70 spectrometer) was used to analyse the functional groups of DSS adsorbents and their changes after the MB adsorption. About 1 mg of sample DSS was mixed with approximately 200 mg of dried KBr to get pellets. Measurements were taken over the range $4000\text{--}400 \text{ cm}^{-1}$ in the absorbance mode, with a spectral resolution of 4 cm^{-1} .

SEM images and EDX compositional data of the DSS powder were acquired using a "Hirox scanning electron microscopy equipped with an Energy Dispersive X-ray analysis system.

The textural characterization of the adsorbent was determined by means of N₂ physisorption at $-196 \text{ }^\circ\text{C}$ using an automatic Autosorb IQ (Quantachrome) analyzer. The DSS samples was degassed at $150 \text{ }^\circ\text{C}$ for 2 h. The generated isotherms were used to calculate their specific surface area (S_{BET}), micro- and mesoporosity. Pore size distribution and the average pore were examined by the Barrett–Joyner–Halenda (BJH) method from the desorption branch of the isotherms. Additionally, the

point of zero charges (pHPZC) of DSS adsorbent was determined by solid addition method [39].

Batch adsorption study

The adsorption experiments were launched by stirring 0.2 g of DSS adsorbent that prepared with 100 mL of the MB dye solution in an orbital shaker (IKAKS control 4000I), controlling the temperature and agitation. Then, all the MB adsorption tests on the DSS were conducted in triplicate. Samples were taken every 10 min within 240 min, and the suspensions were centrifuged at 5000 rpm for 5 min and filtered through $0.45 \text{ }\mu\text{m}$ membrane filters (Durapore®-Millipore). The measurements of adsorbate concentrations are made by UV–visible spectrophotometer (Varian Cary® Type 50) at a maximum wavelength of 664 nm. The adsorption capacity of MB uptake at equilibrium (Q_e) was calculated by using Eq. (1).

$$Q_e = \frac{(C_i - C_e) \times V}{m} \quad (1)$$

where Q_e is the amount of MB adsorbed by the sorbent mg L^{-1} , C_i is the initial liquid-phase concentration of MB mg/L^{-1} , C_e is the liquid-phase concentration of MB mg L^{-1} at equilibrium, V is the solution volume (L) and m is the mass of the adsorbent used (g).

Adsorption kinetics and adsorption isotherms

Cationic MB dye adsorption kinetics was performed using the batch equilibration system, from 5 to 240 min, for a dye concentration from 2.5 mg L^{-1} to 50 mg L^{-1} at $20 \text{ }^\circ\text{C}$. Different mathematical models (nonlinear regression, PFO and PSO kinetic equations) were using for the fitting of the experimental data. The mathematical expressions of these two kinetic models have been expressed as follows (2), (3).

Pseudo first-order model

$$q_t = q_e(1 - e^{-k_1 t}) \quad (2)$$

where q_t is the amount of MB adsorbed per unit mass of adsorbent mg g^{-1} at time t , k_1 is the PFO rate constant L min^{-1} , and t is the contact time (min) [43].

Pseudo second-order model

$$q_t = \frac{q_e^2 k_2 t}{1 + q_e k_2 t} \quad (3)$$

where $k_2 \text{ g (mg min)}^{-1}$ is the rate constant for adsorption, $q_e \text{ mg g}^{-1}$ the amount of MB adsorbed at equilibrium and $q_t \text{ mg g}^{-1}$ is the amount of MB adsorbed at time t [43].

Langmuir isotherm

The Langmuir isotherm assumes that homogeneous monolayer adsorption occurs on the surface of the adsorbent can be expressed as set out in the Eq. (4)

$$q_e = \frac{q_m K_L C_e}{1 + K_L C_e} \quad (4)$$

In the non-linear equation above, the K_L (Lg^{-1}) is the Langmuir equilibrium constant and q_m ($mg\ g^{-1}$) is about the maximum monolayer saturation capacity obtained from the theoretical Langmuir model. Whilst, q_e ($mg\ g^{-1}$) is the adsorption capacity of MB and C_e is the MB concentration remaining in solution at equilibrium respectively, in all the equations listed [43].

Freundlich isotherm model

The Freundlich isotherm model described the adsorption on the heterogeneous surface of the adsorbent and this through a multilayer adsorption mechanism. As well, the non-linear form of Freundlich model is expressed as follows Eq. (5).

$$q_e = K_F C_e^{1/n} \quad (5)$$

K_F (mg/g (L/mg) $^{0.1/n}$) is the Freundlich constant and n is the heterogeneity factor indicating the adsorption intensity [43].

Sips isotherm model

The Sips model is the implementation of a combination of the Langmuir and Freundlich models, used to predict adsorption in heterogeneous systems.

$$q_m = \frac{q_s K_s C_e^\gamma}{1 + K_s C_e^\gamma} \quad (6)$$

where q_m the Sips maximum adsorption capacity ($mg\ g^{-1}$), K_s the Sips equilibrium constant ($L\ mg^{-1}$) and n the Sips model exponent describing heterogeneity [39].

The essential feature of the Langmuir isotherm can be expressed in terms of a dimensionless constant called separation factor R_L , also called equilibrium parameter, which is defined by the Eq. (7):

$$R_L = \frac{1}{(1 + k_L C_0)} \quad (7)$$

where C_0 ($mg\ L^{-1}$) is the higher initial adsorbate concentration. The value of R_L indicates the shape of the isotherms to

be either unfavourable ($R_L > 1$), linear ($R_L = 1$), favourable ($0 < R_L < 1$) or irreversible ($R_L = 0$).

The R^2 analysis was used to fit experimental data with adsorption kinetic and isotherm. The fit appreciation was assessed by the coefficient of determination R^2 , which is given by the Eq. (8).

$$R^2 = 100 \left(1 - \frac{\|q_{exp} - q_{mod}\|^2}{\|q_{exp} - q_{avr}\|^2} \right) \quad (8)$$

where q_{exp} ($mg\ g^{-1}$) is equilibrium capacity from the experimental data, q_{avr} ($mg\ g^{-1}$) is equilibrium average capacity from the experimental data and q_{mod} ($mg\ g^{-1}$) is equilibrium from model. So that $R^2 \leq 100$, the closer the value is to 100, the more perfect is the fit.

Results and discussion

Characterization of adsorbent

The SEM micrograph examination (Fig. 1a) of the DSS samples showed that the structure was relative compact with some concavity and there are virtually no pores of the material. The obtained results were in correlation with previously reported works [20, 44]. The Energy Dispersive ED X-ray spectrometer (Fig. 1S), revealed the presence of oxygen, silicon, carbon and calcium minerals as major components. (Fig. 1b) collects the N_2 adsorption–desorption isotherms obtained of DSS. As can be seen a typical type II isotherm indicates the macro porous characteristics of the adsorbents according to the IUPAC classification. The surface area of the DSS is $24.42\ m^2\ g^{-1}$ found it by using BET method. With the Barrett–Joyner–Halenda (BJH) method, we found that the cumulative pore volume was about $0.059\ cm^3\ g^{-1}$ and Micropore volume is $0.001\ cm^3\ g^{-1}$. (Table 1 and Fig. 1b). The organic matter fraction of the DSS is about 30 wt. %, (7.48% Moisture, 31.64% Volatiles matter and 60.88% Ash). The Bulk density is $0.65\ g\ mL^{-1}$, and 6.7 for pH_{pzc} (Fig. 2).

The obtained FTIR spectra before and after adsorption of MB onto DSS is given in Fig. 1c that shows many functional groups present on the adsorbent surface. There are intense, readable and individualized adsorption bands at $2850\ cm^{-1}$ and $2920\ cm^{-1}$ that can attributed to the C-H in methyl and methylene groups, respectively. The weak band at $1650\ cm^{-1}$ related to C=O stretching of ketones, aldehydes, lactones or carboxyl groups; which becomes moderately intense after MB adsorption. The vibration band of C=C at $1430\ cm^{-1}$ become small after MB adsorption. The most intense bands are perfectly observed at $1050\ cm^{-1}$ in the spectra of DSS can be attributed to Si–O–Si or Si–O–C

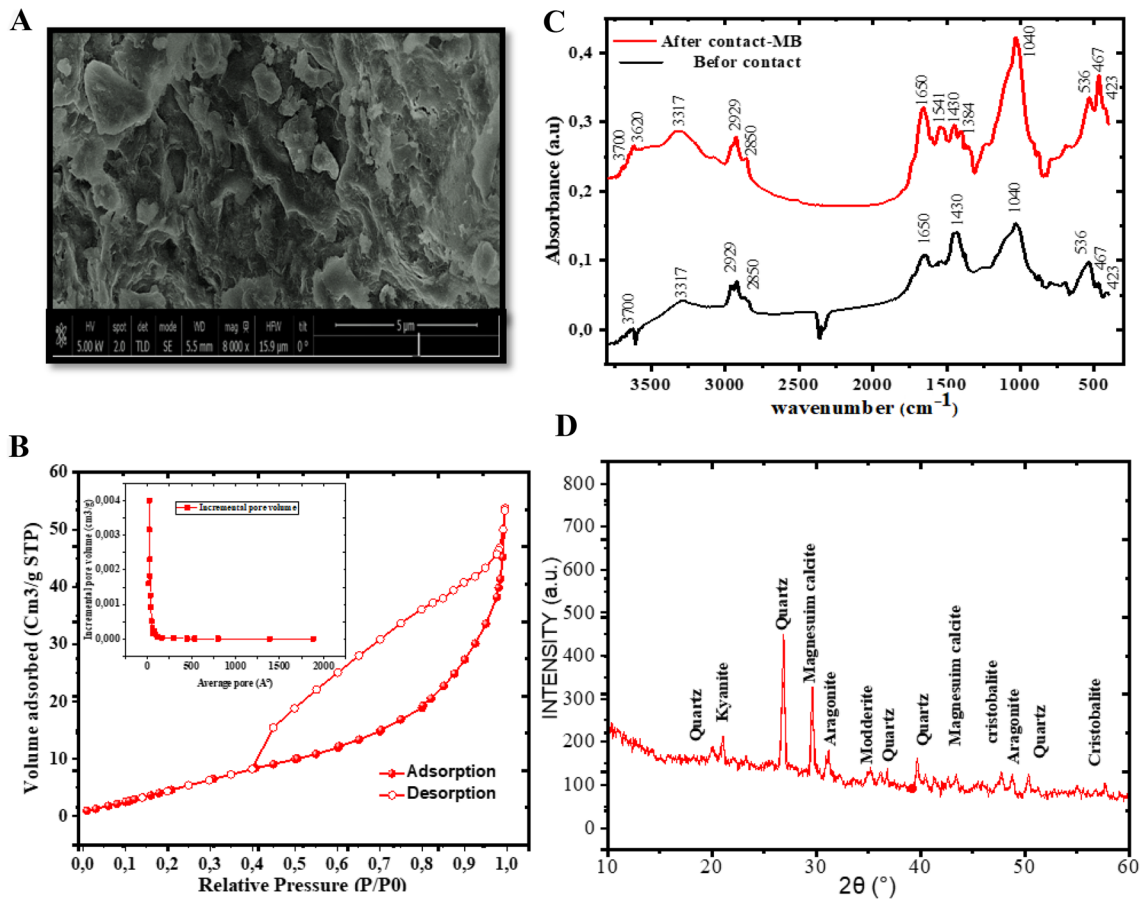


Fig. 1. a SEM image of DSS; b Nitrogen adsorption/desorption Isotherm plot of DSS and Pore sizes distribution of the sample given with BJH method; c FTIR spectra corresponding to the powdered

DSS sample, before and after BM adsorption; d X-ray diffractogram of the deride sewage sludge used

Table 1 Textural data of the investigated sample as estimated from N₂ physisorption

| Sample | S _{BET} (m ² /g) | Total pore volume (cm ³ /g) | Micropore volume (cm ³ /g) |
|--------|--------------------------------------|--|---------------------------------------|
| DSS | 24.420 | 0.059 | 0.001 |

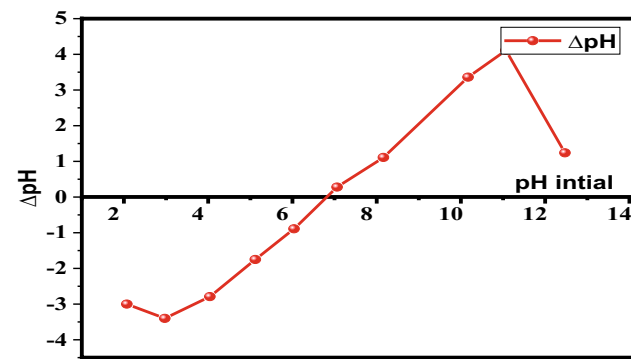


Fig. 2 Point of zero charge of DSS

structures, which is associated with the silicon content of the sewage sludge as confirmed by the ED-X-ray spectra. According to Li et al., (2020), only the intensity of the peak changed before and after the adsorption, indicating that the adsorption of MB is a physical adsorption [45]. However, in our study although the intensity of the peak changed before and after the adsorption, some peaks appear after MB adsorption such as 1451 cm⁻¹ and 1384 cm⁻¹ indicating that the adsorption of MB is a chemical adsorption.

XRD patterns of the DSS (Fig. 1d and Fig. 0.3S) shows that quartz (SiO₂) and calcite (CaCO₃) are the two phases identified in the majority, with the presence of other minority phases. Then, Quartz (Ref. Code:01-083-2468) is identified by its characteristic peaks at *d*=4.25 Å; 3.34 Å; 2.45 Å (very intense) and 1.81 Å. Carbonates are represented by aragonite (4.67 Å; 3.28 Å) and magnesium calcite (Ref. Code: 01-089-1306) at (3.83 Å).

Batch adsorption studies

Effect of adsorbent amount

The effect of DSS adsorbent amount on the adsorption efficiency was studied. The variation of adsorbent amount in the range (0.05–8 g) at a fixed MB concentration (10 mg L⁻¹) for MB removal by DSS is shown in (Fig. 3a). The results show that initially, a rapid increase in the adsorption capacity, with the increase in adsorbent amount. This can be attributed to the greater surface area and the high number of activated sites available. After the critical concentration, (0.2 g, at which is about 90% of the dye becomes adsorbed) the adsorption rate is progressively reduced until the maximum value of about 97% adsorption is reached in the DSS sample.

Effect of contact time and initial concentration

The contact time is an important issue in adsorption, which is mainly an equilibrium process, and determining the equilibrium time. The effect of contact time and the initial

concentration on removal of MB (2.5, 5, 10, 20, 30 and 50 mg L⁻¹) into DSS are shown in (Fig. 3b). The results of the contact time effect have been shown that the adsorption capacity increased with the increase of contact time and reach equilibrium in 150 min for all concentrations. The adsorption was rapid within the first 100 min then continued at a low speed until it reached equilibrium. The rapid initial phase was probably due to the abundance or presence of active sites, could be due to physical adsorption or ion exchange on the surface of the adsorbent [46]. The adsorption became less effective at the slowest stage due to the decrease in active sites on the surface of adsorbent.

Effect of pH

The pH of the solution is one of the most important factors influencing the adsorption capacity of an adsorbent. In addition to its effect on the degree of deprotonation and speciation of the surface functional groups on the adsorbent, it can also affect the state of the adsorbate. This subsequently leads to a shift in reaction kinetics and equilibrium characteristics of adsorption process. The effect of pH value

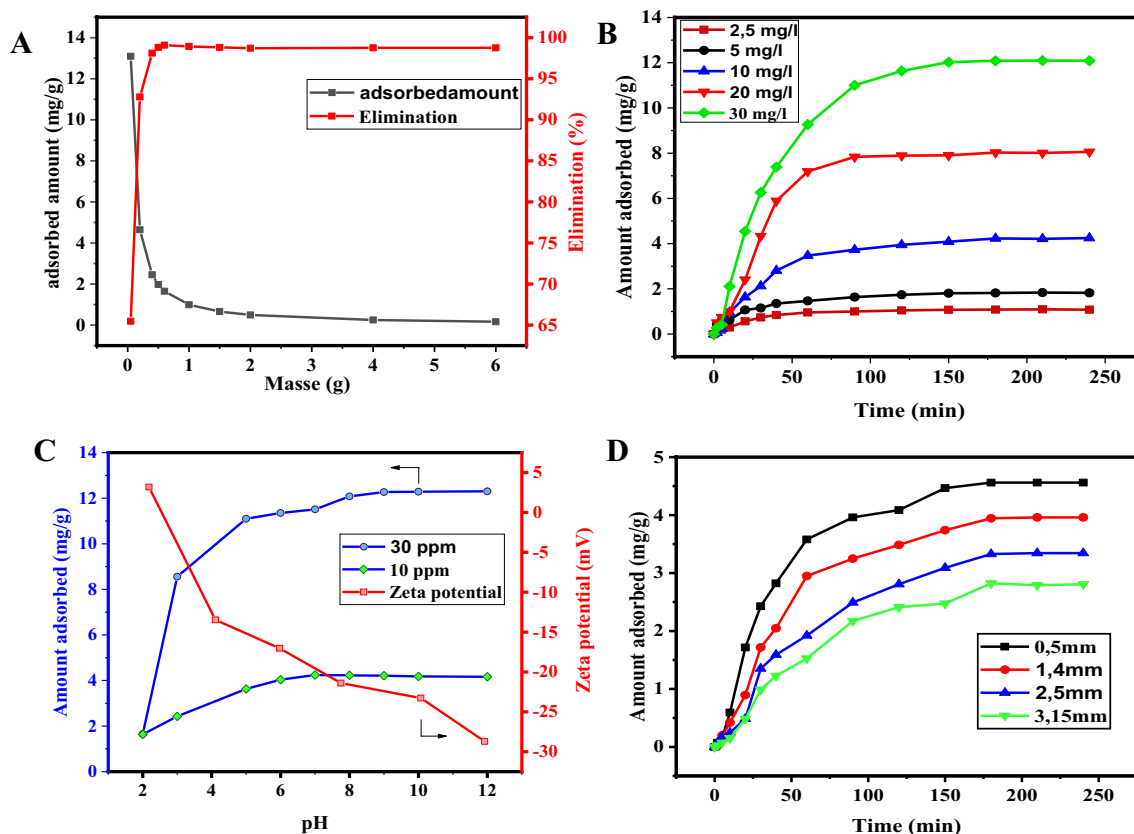


Fig. 3. a Effect of adsorbent dosage on retention of MB by DSS sample; b Effect of contact time and initial concentration of MB adsorption onto DSS ($V = 100$ mL, $T = 20$ °C, shaking speed = 150 rpm and 0.2 g of DSS). c Effect of initial pH on MB removal, using 0.2 g

of DSS, $[MB]_i = 10$ mg/L and 30 mg/L and zeta potential of DSS as function of pH. d The effect of particle size to the adsorption rate of MB on DSS using 0.2 g of DSS, $[MB]_i = 10$ mg/L, $V = 100$ mL, $T = 20$ °C, $pH = 6,9$, shaking speed = 150 rpm

on sorption experiments was examined over a range of pH from 2 to 12 at MB initial concentrations of 30 mg L^{-1} and 10 mg L^{-1} . As shown in Fig. 3c, it is clear that MB removal efficiency increased significantly in the pH range between 2 and 7. Then the behavior changed insignificantly, it becomes considerably constant in the pH range from 8 to 12. This adsorption behavior is consistent with several works cited in the literature [47, 48]. The highest adsorption capacity was observed at pH 9 for DSS. Indeed, the pH-dependent adsorption behavior of MB can be explained with respect to the point of zero charge (pHzpc) of adsorbent. The point zero charge (pHzpc) of DSS was found at pH equal to 6.9 (Fig. 2). It is remarkable that at low solution pH, the DSS surface protonated and acquired a positive charge, which is confirmed by the zeta potential measurement. Thus an electrostatic repulsion occurred between the cationic MB dye and the positively charged active sites of the adsorbent, leading to a reduction of the adsorption capacity. However, at solution pH value was greater than pHzpc, the DSS surface becomes more deprotonated and acquired a negative charge, as well as a strong electrostatic attraction between the cationic MB dye and the negatively charged active sites of the DSS adsorbent, which led to an increase in adsorption capacity of MB.

Effect of particles size

In general, the adsorption capacity is affected by the particle size of adsorbent. The adsorption kinetics has been studied for the different powder granules ranging from 0.5 mm to more than 3.15 mm. Figure 3d Shows that the amount adsorbed of MB increases as the particle size decreases. This is explained by the fact that the finer the particle size, the greater the specific surface area, the greater the adsorption [49, 50].

Effect of ionic strength

Industrial wastewater contains significant amounts of salts, several studies on dye adsorption have shown that the ability to adsorb dyes is strongly influenced by the nature and concentration of electrolytic ionic elements added to the dye bath. The effect of inorganic salt (NaCl) on adsorption rate of MB on DSS was examined by adding concentration of NaCl in the range of $0.1\text{--}0.005 \text{ mol L}^{-1}$, the obtained result is presented in Fig. 4), as seen the presence of NaCl salt has influenced the adsorption capacity of MB. The dye adsorption lightly decreases with the increasing of salt concentration. This result is in coherence with those reported by other authors [47, 51]. Therefore, the salt screens the electrostatic interaction of opposite charges of the surface and the dye molecule, the adsorbed amount should decrease with

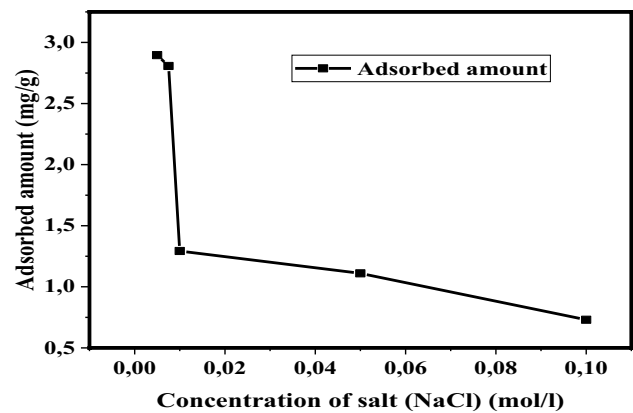


Fig. 4 The effect of ionic strength to the adsorption rate of MB on DSS using 0,2g of DSS, [MB]_i = 10 mg/L, $V = 100 \text{ mL}$, $T = 20 \text{ }^\circ\text{C}$, pH=6,9, shaking speed = 150 rpm

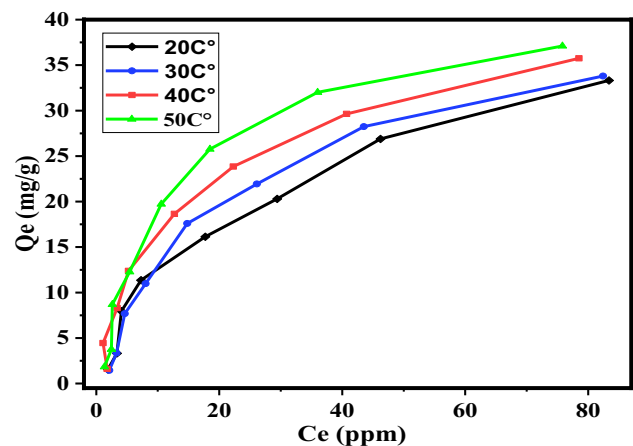


Fig. 5 The effect of temperature to the adsorption rate of MB on DSS using 0,2g of DSS, [MB]_i = 10 mg./L, $V = 100 \text{ mL}$, pH=6,9, shaking speed = 150 rpm

increase of NaCl concentration. Our results contradict those obtained by other author [52].

Effect of temperature

In order to determine the optimal temperature of the process the adsorption of MB into DSS the experiments were carried out at 20, 30, 40 and $50 \text{ }^\circ\text{C}$, the results of these experiments are shown in (Fig. 5) It was observed that as the temperature increased, the adsorption capacity also increased and the optimal temperature it $50 \text{ }^\circ\text{C}$. The enhancement in adsorption with temperature may be due to the increase in the dye mobility required to penetrate the sample pores at high temperatures, the increase in the chemical interactions between the adsorbate and the surface functionalities of the adsorbent, the change in chemical potentials, related to the

solubility of the adsorbate species. Therefore, as the temperature increases, the solubility increases and the chemical potential decreases. Thus, both the effects, the solubility and the normal temperature effects, work in the same direction. The adsorption reaction at any interface between two phases can be regarded as an equilibrium process. This suggests that the adsorption process is endothermic in nature [53].

Kinetics study

The kinetic study presents a high important in the adsorption study, which gives an idea of adsorbate uptake rate and efficiency of adsorption. The mechanism of adsorption depends upon the physical and chemical characteristics of the adsorbent as well as the mass transfer process. The kinetics of adsorption of MB dye onto DSS was performed by withdrawing and analysing the samples at the time interval of every 5 min for the first 10 min and later at every 10 min until the consecutive residual dye concentrations became closer. The kinetic experiments were carried out separately for six different initial dye concentrations such as 2.5, 5, 10, 20, 30 and 50 mg L⁻¹ for the particle size 0.5 mm of adsorbent, at 293 K. The experiments were carried out by adjusting the initial pH of the solutions at 6.9. Experiments with increasing contact times, ranging from 5 to 250 min, were carried out.

The adsorption kinetics data are fitted to the PFO and PSO using non-linear regression. The experimental equilibrium data and the predicted theoretical kinetics for the adsorption of MB onto DSS are presented in Fig. 6. From these results (Table 2), the PSO model is more adapted to describe the adsorption dynamics of the cationic dye MB on the DSS due to the good correlation parameters calculated by the model with experimental data ($R^2=0.99$), this suggested that boundary layer resistance was not the rate limiting step [54]. The rate of adsorption may be controlled largely by a chemisorption process, in conjunction with the chemical characteristics of the adsorbent and dye molecules.

Adsorption isotherm

Figure 7 shows MB adsorption experimental data together with values predicted by the three adjustment models used. Equations (4), (5) and (6) represent Langmuir, Freundlich and Sips models and their respective parameters for this study are shown in Table 3, along with determination coefficients.

In this study, regarding the isotherms fittings for data of sample considered, as seen in Table 3, quite high correlation coefficients ($R^2 > 0.9$) were found for both models; nevertheless, Langmuir model seems to provide slightly better fittings than the Freundlich one. The Langmuir model is used in MB adsorption with Red-clay and Rhassoul-clay [55], in

all cases, adequate adjustment was obtained for experimental data. In our study Langmuir model represented DSS adsorptive process with quality.

In the Freundlich isotherm model, the value of n indicates the type of isotherm. When $0 < 1/n < 1$, the adsorption is favourable; when $1/n = 1$, the adsorption is irreversible; and when $1/n > 1$, the adsorption is unfavourable. In this study, the $1/n$ value is 0, 53 less than 1, so condition for removal of MB into DSS. Indeed, we used the Sips equation, since parameter ns indicates favourable how much the adsorbent surface is heterogeneous as it deviates from unity. Nethaji et al. used Sips equation in cationic and anionic dyes adsorption onto carbonaceous particles prepared from Juglans Regia shell biomass and obtained good fitting [56]. For DSS, the ns value gets closer to unity, indicating a surface approximately homogeneous.

Adsorption thermodynamics

In the adsorption process the thermodynamic parameters, such as the change in enthalpy (ΔH°), entropy (ΔS°) or Gibbs free energy (ΔG°), are important, as indicators for the practical application of a process [57]. The values of these parameters provide information regarding the spontaneity and viability of a system. According to the latest estimates and suggestion of Eder-Lima et al. (2019) for improving the correct way to determine thermodynamic parameters for adsorption equilibrium [39, 58].

The ΔH° and ΔS° values can be determined from the slope and the intercept of the $\ln Ke^\circ$ against $1/T$ (Fig. 8), where $ke^\circ = \frac{1000 \cdot K_L \cdot \text{molecular weight of adsorbate} \cdot [\text{adsorbate}]^\circ}{[\text{adsorbate}]^\circ}$, (Ke° is the thermodynamic equilibrium constant that is dimensionless, K_L is the Langmuir isotherm constant, $[\text{adsorbate}]^\circ$ is the standard concentration of the adsorbate (1 mol/L mol L⁻¹), and γ is the activity coefficient which is unitary for very diluted or ideal solutions). The ΔG° value can be determined from Eq. (10).

$$\ln ke^\circ = -\frac{\Delta H^\circ}{RT} + \frac{\Delta S^\circ}{R} \quad (9)$$

$$\Delta G^\circ = \Delta H^\circ - T\Delta S^\circ \quad (10)$$

In this study, the experiments were carried out at four temperatures (293, 303, 313 and 323 K), with eight systems containing different concentrations of MB dye, generating four Ke° values to be inserted into Eq. (9) in order to plot $\ln Ke^\circ$ versus $1000 \cdot T^{-1}$.

As can be seen in Table 4, the negative ΔG° value indicates that the process spontaneous with increasing temperature, the ΔH° value is positive confirming the endothermic nature of the adsorption process. Hence, the positive value

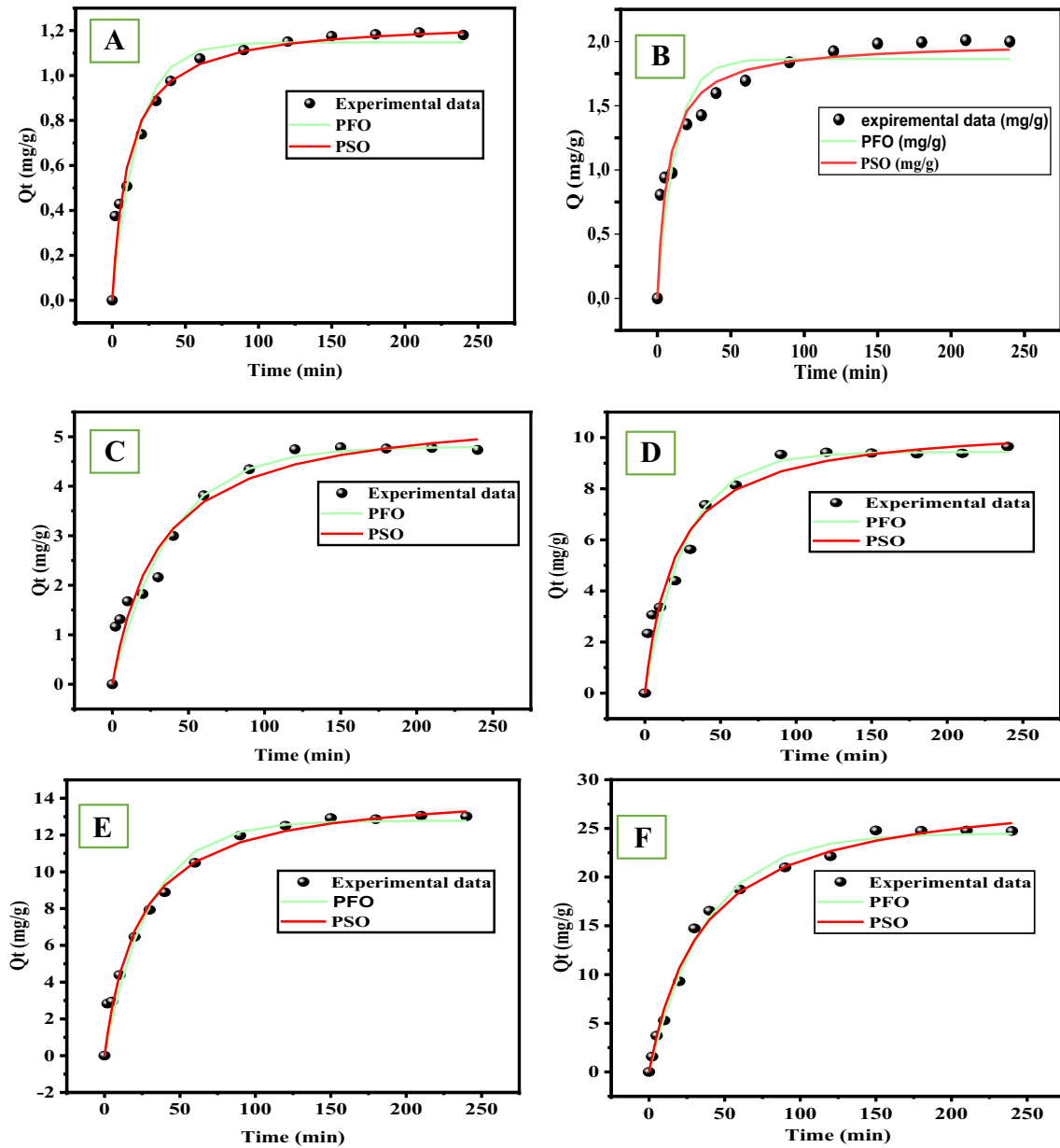


Fig. 6 PFO and PSO nonlinear for DSS with initial concentration 2.5 mg/L (a), 5mg/L (b), 10 mg/L (c), 20 mg/L (d), 30 mg/L (e) and 50 mg/L (f)

Table 2 Non-linear regression kinetic model parameters for the studied dsye

| C ₀ mg/l | PFO | | | PSO | | | |
|---------------------|--------------------|---------------------|------------------------|--------------------|----------------|---------------------------|--------------------|
| | Q _{e,exp} | Q _{e,calc} | K ₁ (1/min) | R ² (%) | Q _e | K ₂ (g/mg*min) | R ² (%) |
| 2.5 | 1.19 | 1.14 | 0.058 | 94 | 1.24 | 0.071 | 97 |
| 05 | 1.99 | 1.84 | 0.081 | 86 | 1.99 | 0.067 | 94 |
| 10 | 4.73 | 4.80 | 0.026 | 94 | 5.58 | 0.005 | 94 |
| 20 | 9.65 | 9.43 | 0.037 | 95 | 10.57 | 0.004 | 96 |
| 30 | 13.00 | 12.78 | 0.033 | 97 | 14.54 | 0.003 | 98 |
| 50 | 24.73 | 24.49 | 0.026 | 99 | 29.25 | 0.001 | 99 |

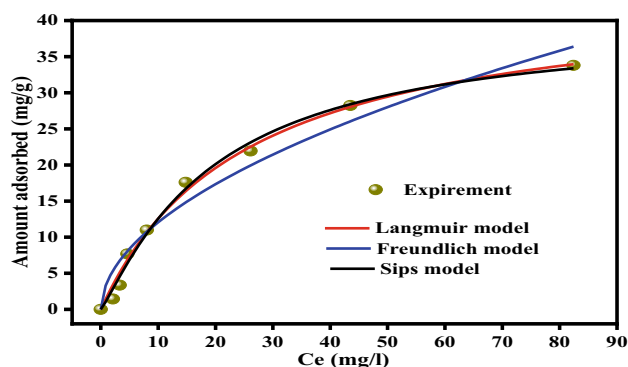


Fig. 7 Langmuir, Freundlich and Sips nonlinear regression for dried sewage sludge adsorbent

Table 3 Parameters of adsorption isotherm models for MB adsorption by the DSS sample

| Langmuir model | | Freundlich model | | Sips model | |
|----------------|-------|------------------|------|------------|-------|
| Q_m | 44.39 | – | – | Q_m | 39.8 |
| K_L | 0.039 | $1/n$ | 0.52 | K_S | 0.032 |
| R_L | 0.33 | K_F | 3.61 | n_S | 1.14 |
| R^2 (%) | 99.05 | R^2 (%) | 94.8 | R^2 (%) | 99.1 |

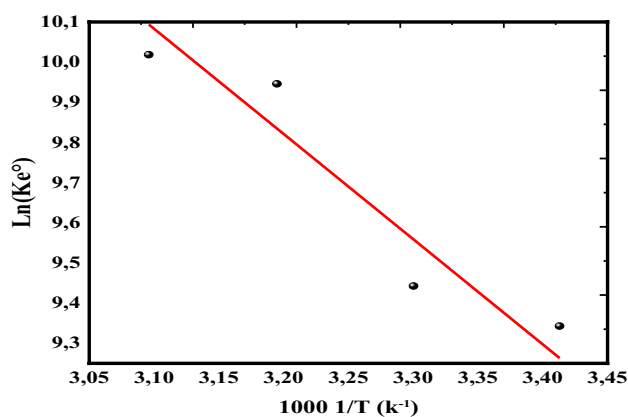


Fig. 8 Thermodynamic study for the MB adsorption on the DSS sample, performed through fitting of the experimental data to the linear form of van't Hoff equation

Table 4 Thermodynamic parameters of the adsorption process of MB onto the DSS adsorbents

| ΔG° (KJ.mol ⁻¹) | | | | ΔH° (KJ.mol ⁻¹) | ΔS° (J.mol ⁻¹ .K ¹) |
|--|--------|--------|--------|--|---|
| 293 K° | 303 K° | 313 K° | 323 K° | 19.90 | 145.26 |
| -22.66 | -24.11 | -25.56 | -27.01 | | |

Table 5 Comparison of maximum adsorption capacities of various types of adsorbents for MB removal

| Adsorbents | q_m (mg g ⁻¹) | S_{BET} (m ² g ⁻¹) | References |
|--|-----------------------------|---|------------|
| Red-clay | 18.83 | 22.4 | [55] |
| Raw Coal fly ash | 5.06 | 8.3 | [62] |
| Activated lignin-chitosan pellets | 36.25 | 80.77 | [63] |
| Raw kaolin | 13.99 | 24 | [64] |
| Raw-ball clay at 30 C° | 25 | 10 | [65] |
| Natural zeolite | 19.9 | 24.59 | [66] |
| Nature cactus | 3.44 | NR | [67] |
| Dried Cactus | 14.04 | NR | |
| Palm kernel fiber | 5.4 | NR | [68] |
| Fe ₃ O ₄ @SiO ₂ -(CH ₂) ₃ -IL/Talc | 6.23 | NR | [69] |
| KMgFe(PO ₄) ₂ | 22.83 | NR | [70] |
| Grass waste | 457,64 | NR | [38] |
| Papaya seeds (PS) | 555,557 | NR | [38] |
| Water hyacinth | 462,9 | NR | [38] |
| DSS | 44.39 | 24.42 | This work |

NR Not reported

of ΔS° indicates an irregular increase in randomness at the DSS-solution interface during adsorption [59]. Our results similar with those published by other authors in recent paper who reported positive values for both ΔH° and ΔS° in the case of the adsorption of MB onto some clays (Red clay and Rhassoul-clay) [55]. On the contrary, our results appear differently in relation to those detailed for similar process over other adsorbents, [60, 61]. In anyway, it is necessary to see it that building up a connection between thermodynamic and the mineralogical nature of the adsorbents of the adsorption process is not surely a simple undertaking task. In a relatively recent article, in which both endo-or exothermic characteristics could be observed for the same type of mineral category.

Comparison of adsorption capacity of DSS adsorbent with other available adsorbents

Adsorption capacity of DSS was correlates with other available adsorbents are indicated in Table 5. The comparison clearly showed that the adsorbent developed is much more effective for the removal of MB dye from aqueous solution compared to some adsorbents previously reported. Although, there are many reported adsorbent with higher adsorption capacity towards MB, they need complicated processes for the activation using acids and corrosives and are time consuming. It is important to note that the preparation of our DSS adsorbent required less energy and has not undergone any chemical modification. Indeed, compared to other adsorbent such as activated lignin-chitosan pellets,

which require a chemical modification, by acetic acid followed by other physics at high temperature that reach 600 °C for 2 h. Another advantage of the developed DSS material is its low-cost as well as it is an environmental friendly. Hence, Activated lignin-chitosan pellets, and the adsorption capacity of DSS 44.39 mg g⁻¹ much better than this for Activated lignin-chitosan pellets 36.25 mg g⁻¹.

Real wastewater test

For more advanced valorization of the studied DSS, the adsorption of a real wastewater effluent containing MB as main dye was studied to evaluate the treatment efficiency. The characteristic of the real wastewater before test are given in Table 1S (Supplementary materials). Adsorption studies were carried out using 50 mg L⁻¹ of MB for 3 h reaction time at 25 °C in the presence of 200 mg of DSS. As can be seen in Fig. 9, the after-treatment measurement shows that 35% of MB is adsorbed. In addition, the removal rate is reduced when comparing the two solutions (synthetic solution and real wastewater solution), which is normal, especially since there are several other elements in the real wastewater solution that causes the inhibition of the adsorbent pores of DSS. This is consistent with the salt effect study mentioned above in Fig. 7.

Conclusions

To conclude, the study of the sorption properties of MB dye, DSS adsorbent were carried out in batch system. Hence, we found that the DSS adsorbent has a good dye retention capacity. The adsorption of MB into DSS was spontaneous and endothermic. The values of the ΔH and the ΔS are

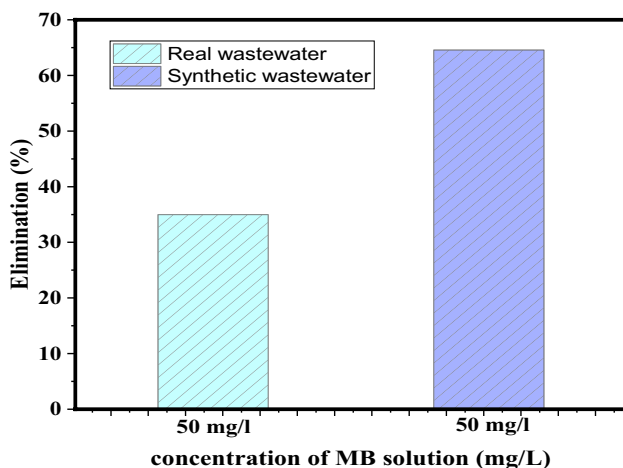


Fig. 9 Histograms of the MB elimination percentage of DSS in real waste water and synthetic wastewater

19.90 kJ/mol and 145.26 J/mol K, respectively. The results obtained indicate that the Langmuir model fitted well with the experimental data and was used to estimate the model parameters. Adsorption kinetics followed the PSO model. The DSS from domestic treatment plant showed a good MB adsorption capacity compared to other clay adsorbents and can be easily prepared without any physical and/or chemical treatment. Adsorption of the cationic MB dye on the sludge surface can be considered as a simple, fast and economical method for its removal from aqueous solutions. Therefore, the DSS material can be successfully applied in WWTPs at a large scale for the removal of the MB. In addition, the DSS can be easily extended for other organic pollutants removal applications.

Supplementary Information The online version contains supplementary material available at <https://doi.org/10.1007/s41204-021-00111-6>.

Acknowledgments The research work was supported by Ministry of Energy, and Mines and the Environment within the Research Project with grant number 018-1212-00019.

Author's contribution AEHAY and AM have contributed equally to this work.

Compliance with ethical standards

Conflict of interest The authors declare that there is no conflict of interest.

References


1. Chanaka Udayanga WD, Veksha A, Giannis A, Lisak G, Chang VWC, Lim TT (2018) Fate and distribution of heavy metals during thermal processing of sewage sludge. *Fuel* 226:721–744
2. Dubis B, Jankowski KJ, Załuski D, Sokólski M (2020) The effect of sewage sludge fertilization on the biomass yield of giant miscanthus and the energy balance of the production process. *Energy* 206
3. Werle S, Wilk RK (2010) A review of methods for the thermal utilization of sewage sludge: the polish perspective. *Renew Energy* 35(9):1914–1919
4. Werle S, Dudziak M (2014) Gaseous fuels production from dried sewage sludge via air gasification. *Waste Manag Res* 32(7):601–607
5. Schnell M, Horst T, Quicker P (2020) Thermal treatment of sewage sludge in Germany: a review. *J Environ Manage* 263:110367.
6. Joo SH, Dello Monaco F, Antmann E, Chorath P (2015) Sustainable approaches for minimizing biosolids production and maximizing reuse options in sludge management: a review. *J Environ Manage* 158:133–145
7. Agabo-García C, Pérez M, Rodríguez-Morgado B, Parrado J, Solera R (2019) Biomethane production improvement by enzymatic pre-treatments and enhancers of sewage sludge anaerobic digestion. *Fuel* 255:115713
8. Rasapoor M, Young B, Brar R, Sarmah A, Zhuang WQ, Baroutian S (2019) Recognizing the challenges of anaerobic digestion: critical steps toward improving biogas generation. *Fuel* 261:116497

9. Lu D, Wu D, Qian T, Jiang J, Cao S, Zhou Y (2020) Liquid and solids separation for target resource recovery from thermal hydrolyzed sludge. *Water Res* 171:115476
10. Collivignarelli MC, Canato M, Abbà A, Carnevale Miino M (2019) Biosolids: what are the different types of reuse? *J Clean Prod* 238.
11. <https://secretariatministre@environnement.gov.ma>, "Ref, [11]," no. January. pp. 2–3, 1976.
12. Lavoie J, Srinivasan S, Nagarajan R (2011) Ref 12. *J Hazard Mater* 194:85–91
13. Belloulid MO, Moussaoui TEL, Saykoug J, Azzouzi FEL, Words KEY (2018) National program of sanitation and wastewater treatment in Morocco: objectives, achievements and challenges programme national d' assainissement liquide et d' épuration des eaux usées au Maroc: objectifs, réalisations et défis. *Environ Water Sci Public Heal Territ Intell* 2(1):67–76
14. Hadi P, Xu M, Ning C, Sze Ki Lin C, McKay G (2015) A critical review on preparation, characterization and utilization of sludge-derived activated carbons for wastewater treatment. *Chem Eng J* 260:895–906
15. Naik PK (2017) Water crisis in Africa: myth or reality? *Int J Water Resour Dev* 33(2):326–339
16. Choukri F et al (2020) Distinct and combined impacts of climate and land use scenarios on water availability and sediment loads for a water supply reservoir in northern Morocco. *Int Soil Water Conserv Res* 8(2):141–153
17. Ahrouch M, Gatica JM, Draoui K, Bellido D, Vidal H (2020) Honeycomb filters as an alternative to powders in the use of clays to remove cadmium from water. *Chemosphere* 259:127526
18. Gorguner M, Kavvas ML (2020) Modeling impacts of future climate change on reservoir storages and irrigation water demands in a Mediterranean basin. *Sci Total Environ* 748:141246
19. Zhang H, et al. (2020) Production of biochar from waste sludge/ leaf for fast and efficient removal of diclofenac, vol. 299. Elsevier B.V.
20. Li WH, Yue QY, Gao BY, Ma ZH, Li YJ, Zhao HX (2011) Preparation and utilization of sludge-based activated carbon for the adsorption of dyes from aqueous solutions. *Chem Eng J* 171(1):320–327
21. Wang M et al (2021) Fabrication of monodispersed plasmonic photocatalysts on activated carbon with the carbon source and reduction property of sewage sludge. *Appl Surf Sci* 538:148036
22. Costa JAS, de Jesus RA, Santos DO, Mano JF, Romão LPC, Paranhos CM (2020) Recent progresses in the adsorption of organic, inorganic, and gas compounds by MCM-41-based mesoporous materials. *Microporous Mesoporous Mater* 291:109698
23. Sellaoui L, et al. (2020) Insights of the adsorption mechanism of methylene blue on brazilian berries seeds: Experiments, phenomenological modelling and DFT calculations. *Chem Eng J* 394
24. Kausar A et al (2019) Preparation and characterization of chitosan/clay composite for direct Rose FRN dye removal from aqueous media: Comparison of linear and non-linear regression methods. *J Mater Res Technol* 8(1):1161–1174
25. Tran HN, et al. (2020) Innovative spherical biochar for pharmaceutical removal from water: insight into adsorption mechanism. *J Hazard Mater* 394: 122255
26. Yazidi A et al (2019) Adsorption of amoxicillin and tetracycline on activated carbon prepared from durian shell in single and binary systems: Experimental study and modeling analysis. *Chem Eng J* 379(July):2020
27. Pang X et al (2020) Preparation and characterization of a novel mountain soursop seeds powder adsorbent and its application for the removal of crystal violet and methylene blue from aqueous solutions. *Chem Eng J* 391:123617
28. Chahinez HO, Abdelkader O, Leila Y, Tran HN (2020) One-stage preparation of palm petiole-derived biochar: Characterization and application for adsorption of crystal violet dye in water. *Environ Technol Innov* 19:100872
29. Ahsaine HA et al (2018) Photo/electrocatalytic properties of nanocrystalline ZnO and La-Doped ZnO: Combined DFT fundamental semiconducting properties and experimental study. *Chem Select* 3(27):7778–7791
30. Anfar Z, El Haouti R, Lhanafi S, Benafqir M, Azougarh Y, El Alem N (2017) Treated digested residue during anaerobic codigestion of Agri-food organic waste: Methylene blue adsorption, mechanism and CCD-RSM design. *J Environ Chem Eng* 5(6):5857–5867
31. Malik PK, Saha SK (2003) Oxidation of direct dyes with hydrogen peroxide using ferrous ion as catalyst. *Sep Purif Technol* 31(3):241–250
32. Silva LGM, et al. (2020) Integration of fenton's reaction based processes and cation exchange processes in textile wastewater treatment as a strategy for water reuse. *J Environ Manage* 272
33. Ciardelli G, Corsi L, Marcucci M (2001) Membrane separation for wastewater reuse in the textile industry. *Resour Conserv Recycl* 31(2):189–197
34. Alventosa-Delara E, Barredo-Damas S, Zuriaga-Agustí E, Alcaina-Miranda MI, Iborra-Clar MI (2014) Ultrafiltration ceramic membrane performance during the treatment of model solutions containing dye and salt. *Sep Purif Technol* 129:96–105
35. Ambaye TG, Hagos K (2020) Photocatalytic and biological oxidation treatment of real textile wastewater. *Nanotechnol Environ Eng* 5
36. Zbair M, Ait Ahsaine H, Anfar Z (2018) Porous carbon by microwave assisted pyrolysis: an effective and low-cost adsorbent for sulfamethoxazole adsorption and optimization using response surface methodology. *J Clean Prod* 202:571–581
37. Badri A, Jabli M, López ML, Ben Amara M (2019) Synthesis, electrical and dye adsorption properties of KZnFe(PO₄)₂ zeolite type structure. *Inorg Chem Commun* 110: 107609
38. Mohammed MA, Shitu A, Ibrahim A (2014) Removal of methylene blue using low cost adsorbent: a review. *Res J Chem Sci* 4(1):91–102
39. Ahrouch M, Gatica JM, Draoui K, Vidal H (2019) Adding value to natural clays as low-cost adsorbents of methylene blue in polluted water through honeycomb monoliths manufacture. *SN Appl Sci* 1:2019
40. Qi Y, Hoadley AFA, Chaffee AL, Garnier G (2011) Characterisation of lignite as an industrial adsorbent. *Fuel* 90(4):1567–1574
41. Yin Q, Liu M, Ren H (2019) Biochar produced from the copyrolysis of sewage sludge and walnut shell for ammonium and phosphate adsorption from water. *J Environ Manage* 249:109410
42. Otero M, Rozada F, Calvo LF, García AI, Morán A (2003) Kinetic and equilibrium modelling of the methylene blue removal from solution by adsorbent materials produced from sewage sludges. *Biochem Eng J* 15(1):59–68
43. Dhaouadi H, M'Henni F (2009) Vat dye sorption onto crude dehydrated sewage sludge. *J Hazard Mater* 164(2–3):448–458
44. Fan S et al (2016) Biochar prepared from co-pyrolysis of municipal sewage sludge and tea waste for the adsorption of methylene blue from aqueous solutions: kinetics, isotherm, thermodynamic and mechanism. *J Mol Liq* 220:432–441
45. Li H, Liu L, Cui J, Cui J, Wang F, Zhang F (2020) High-efficiency adsorption and regeneration of methylene blue and aniline onto activated carbon from waste edible fungus residue and its possible mechanism. *RSC Adv* 10(24):14262–14273
46. Sawasdee S, Jankerd H, Watcharabundit P (2017) Adsorption of dyestuff in household-scale dyeing onto rice husk. *Energy Procedia* 138:1159–1164
47. Mouni L, et al. (2018) Removal of methylene blue from aqueous solutions by adsorption on kaolin: kinetic and equilibrium studies. *Appl Clay Sci* 153:38–45

48. Cheng J et al (2020) Highly efficient removal of methylene blue dye from an aqueous solution using cellulose acetate nanofibrous membranes modified by polydopamine. *ACS Omega* 5(10):5389–5400
49. Abdallah M, Hijazi A, Hamieh M, Alameh M, Toufaily J, Rammal H (2016) étude de l'adsorption du Bleu de Méthylène sur un biomatériau à base de l'eucalyptus selon la taille des particules. *J Mater Environ Sci* 7(11):4036–4048
50. Barka N, Abdennouri M, Makhfouk MEL (2011) Removal of methylene blue and eriochrome black T from aqueous solutions by biosorption on *Scolymus hispanicus* L.: Kinetics, equilibrium and thermodynamics. *J Taiwan Inst Chem Eng* 42(2):320–326
51. Rida K, Bouraoui S, Hadnine S (2013) Adsorption of methylene blue from aqueous solution by kaolin and zeolite. *Appl Clay Sci* 83–84:99–105
52. Malekbala MR, Khan MA, Hosseini S, Abdullah LC, Choong TSY (2015) Adsorption/desorption of cationic dye on surfactant modified mesoporous carbon coated monolith: equilibrium, kinetic and thermodynamic studies. *J Ind Eng Chem* 21:369–377
53. Djilani C et al (2015) Adsorption of dyes on activated carbon prepared from apricot stones and commercial activated carbon. *J Taiwan Inst Chem Eng* 53:112–121
54. Elmoubarki R et al (2015) Adsorption of textile dyes on raw and decanted Moroccan clays: kinetics, equilibrium and thermodynamics. *Water Resour Ind* 9:16–29
55. Bentahar Y, Draoui K, Hurel C, Ajouyed O, Khairoun S, Marmier N (2019) Physico-chemical characterization and valorization of swelling and non-swelling Moroccan clays in basic dye removal from aqueous solutions. *J African Earth Sci* 154:80–88
56. Nethaji S, Sivasamy A, Mandal AB (2013) Adsorption isotherms, kinetics and mechanism for the adsorption of cationic and anionic dyes onto carbonaceous particles prepared from *Juglans regia* shell biomass. *Int J Environ Sci Technol* 10(2):231–242
57. Chen H, Zhao J, Wu J, Dai G (2011) Isotherm, thermodynamic, kinetics and adsorption mechanism studies of methyl orange by surfactant modified silkworm exuviae. *J Hazard Mater* 192(1):246–254
58. Lima EC, Hosseini-Bandegharai A, Moreno-Piraján JC, Anastopoulos I (2019) A critical review of the estimation of the thermodynamic parameters on adsorption equilibria. Wrong use of equilibrium constant in the Van't Hoof equation for calculation of thermodynamic parameters of adsorption. *J Mol Liq* 273:425–434
59. Lebkiri I et al (2019) Removal of methylene blue dye from aqueous solution using a superabsorbent hydrogel the polyacrylamide: Isotherms and kinetic studies. *Mediterr J Chem* 9(5):337–346
60. Xia Yang C, Lei L, Xin Zhou P, Zhang Z, Qiang Lei Z (2015) Preparation and characterization of poly(AA co PVP)/PGS composite and its application for methylene blue adsorption. *J Colloid Interface Sci* 443: 97–104
61. Sakin Omer O, Hussein MA, Hussein BHM, Mgaidi A (2018) Adsorption thermodynamics of cationic dyes (methylene blue and crystal violet) to a natural clay mineral from aqueous solution between 293.15 and 323.15 K. *Arab J Chem* 11(5): 615–623
62. Li H, Dai M, Dai S, Dong X, Li F (2018) Methylene blue adsorption properties of mechanochemistry modified coal fly ash. *Hum Ecol Risk Assess* 24(8):2133–2141
63. Albadarin AB, Collins MN, Naushad M, Shirazian S, Walker G, Mangwandi C (2017) Activated lignin-chitosan extruded blends for efficient adsorption of methylene blue. *Chem Eng J* 307:264–272
64. Brindley GW, Thompson TD (1970) Methylene blue absorption by montmorillonites. Determinations of surface areas and exchange capacities with different initial cation saturations (clay-organic studies XIX). *Isr J Chem* 8(3):409–415
65. Auta M, Hameed BH (2012) Modified mesoporous clay adsorbent for adsorption isotherm and kinetics of methylene blue. *Chem Eng J* 198–199:219–227
66. Han R, Zhang J, Han P, Wang Y, Zhao Z, Tang M (2009) Study of equilibrium, kinetic and thermodynamic parameters about methylene blue adsorption onto natural zeolite. *Chem Eng J* 145(3):496–504
67. Sakr F, Alahiane S, Sennaoui A, Dinne M, Bakas I, Assabbane A (2020) Removal of cationic dye (Methylene Blue) from aqueous solution by adsorption on two type of biomaterial of South Morocco. *Mater Today Proc* 22: 93–96
68. El-Sayed GO (2011) Removal of methylene blue and crystal violet from aqueous solutions by palm kernel fiber. *Desalination* 272(1–3):225–232
69. Alizadeh A, Fakhari M, Safaei Z, Khodeai MM, Repo E, Asadi A (2020) Ionic liquid-decorated Fe₃O₄@SiO₂ nanocomposite coated on talc sheets: An efficient adsorbent for methylene blue in aqueous solution. *Inorg Chem Commun* 121:108204
70. Badri A, Alvarez-Serrano I, Luisa López M, Ben Amara M (2020) Sol-gel synthesis, magnetic and methylene blue adsorption properties of lamellar iron monophosphate KMgFe(PO₄)₂. *Inorg Chem Commun* 121:108217.

Publisher's Note Springer Nature remains neutral with regard to jurisdictional claims in published maps and institutional affiliations.

Authors and Affiliations

Youssef Aoulad El Hadj Ali¹  · Mohammadi Ahrouch^{2,3} · Abdellatif Ait Lahcen⁴ · Abdoulaye Demba N'diaye⁵ · Farida El Yousfi¹ · Mostafa Stitou¹

¹ Laboratoire de L'Eau, Les Etudes Et Les Analyses Environnementales, Département de Chimie, Faculté Des Sciences, Université Abdelmalek Essaadi, Mhannech II, B.P. 2121, 93002 Tétouan, Morocco

² Laboratoire Matériaux Et Systèmes Interfaciaux LMSI, Faculté Des Sciences, Université Abdelmalek Essaadi, Mhannech II, B.P. 2121, 93002 Tétouan, Morocco

³ Departamento C.M., I.M. Y Química Inorgánica, Universidad de Cádiz, 11510 Puerto Real, Spain

⁴ Advanced Membranes and Porous Materials Center, King Abdullah University of Science and Technology (KAUST), Thuwal, Saudi Arabia

⁵ Laboratoire de Chimie, Service de Toxicologie Et de Contrôle de Qualité, Institut National de Recherches en Santé Publique, BP 695, Nouakchott, Mauritanie